

## Luminescence dynamics in Ga(AsBi)

Sebastian Imhof,<sup>1,a)</sup> Christian Wagner,<sup>1</sup> Angela Thränhardt,<sup>1</sup> Alexej Chernikov,<sup>2</sup> Martin Koch,<sup>2</sup> Niko S. Köster,<sup>2</sup> Sangam Chatterjee,<sup>2</sup> Stephan W. Koch,<sup>2</sup> Oleg Rubel,<sup>3,4</sup> Xianfeng Lu,<sup>5</sup> Shane R. Johnson,<sup>5</sup> Daniel A. Beaton,<sup>6</sup> and Thomas Tiedje<sup>7</sup>

<sup>1</sup>*Institut für Physik, Technische Universität Chemnitz, 09107 Chemnitz, Germany*

<sup>2</sup>*Fachbereich Physik, Philipps-Universität Marburg, 35032 Marburg, Germany*

<sup>3</sup>*Thunder Bay Regional Research Institute, Thunder Bay, Ontario P7A 7T1, Canada*

<sup>4</sup>*Department of Physics, Lakehead University, Thunder Bay, Ontario P7B 5E1, Canada*

<sup>5</sup>*Department of Electrical Engineering, Arizona State University, Tempe, Arizona 85287-6206, USA*

<sup>6</sup>*Department of Physics and Astronomy, University of British Columbia, Vancouver, British Columbia V6T 1Z4, Canada*

<sup>7</sup>*Department of Electrical and Computer Engineering, University of Victoria, Victoria, British Columbia V8W 3P6, Canada*

(Received 7 February 2011; accepted 31 March 2011; published online 18 April 2011)

The temporal evolution of the spectrally resolved luminescence is measured for a Ga(AsBi) sample at low temperatures. The results are analyzed with the help of kinetic Monte Carlo simulations incorporating two disorder scales attributed to alloy disorder and Bi-clustering. An average time of 5 ps is identified as the upper limit for carrier capture into the Bi clusters whereas the extracted hopping rate associated with alloy fluctuations is much faster than the transitions between the individual cluster sites. © 2011 American Institute of Physics. [doi:10.1063/1.3580773]

Bismuth-containing semiconductors have recently attracted an increasing interest for several reasons. The incorporation of Bi into GaAs strongly reduces the band gap by around 60–80 meV per percent of Bi.<sup>1–3</sup> Therefore, Ga(AsBi) is regarded as a suitable active material for GaAs-based laser diodes emitting in the telecom wavelength region.<sup>4</sup> Recent results show that only the valence band of GaAs is affected by alloying it with Bi.<sup>5</sup> Thus, Ga(AsBi) offers a unique option for independent valence band engineering in optical devices. In particular, the incorporation of Bi results in a huge shift in the splitoff band, offering a reduction in Auger losses as well as opening up opportunities for the design of spintronic devices.<sup>6</sup>

The epitaxial growth of Ga(AsBi) on GaAs is very challenging due to the high lattice mismatch between GaAs and GaBi as well as the metallic character of Bi.<sup>7</sup> Nevertheless, high-quality crystals containing up to 10% Bi have been reported.<sup>8</sup> However, disorder effects are always present in compound materials as a result of fundamental thermodynamics. Spatial fluctuations of the Bi concentration lead to local fluctuations of the band gap.<sup>9</sup> Therefore, the electronic density of states (DOS) is broadened and includes localized states on the low energy side of the average band gap. Again, the broadening is caused mainly by the fluctuations of the valence band since the incorporation of Bi hardly affects the conduction band states.

In this letter, we quantify the disorder by analyzing experimentally obtained photoluminescence (PL) dynamics using a kinetic Monte Carlo simulation.<sup>10</sup> The main advantage of the time-resolved study is the possibility to identify individual disorder parameters which are only accessible as products of pairs for a time-integrated analysis. The sample under investigation is an epitaxially grown Ga(AsBi) layer with a Bi content around 4%–5%. It is excited quasiresonantly at 1.38 eV using 100 fs pulses with an incident photon

flux of  $4 \times 10^{12} \text{ cm}^{-2} \text{ s}^{-1}$  and a streak-camera is used for detection. All details concerning the growth conditions are given in Ref. 8 and for the experimental setup in Ref. 11.

The theoretical approach is based on a kinetic Monte Carlo algorithm. It has been successfully applied to reproduce both time-resolved<sup>12</sup> and time-integrated spectra,<sup>13,14</sup> in particular also for the Ga(AsBi)/GaAs material system.<sup>11</sup> Here, this model is based on the assumption that the valence band disorder results in a landscape of localized states. Electron-hole pairs can perform phonon-assisted transitions between different localized states, so-called hops. Hence, in the case of low carrier densities, they move independently through the fluctuating lattice potential. The hopping rate for the transition between different sites is defined similarly to Refs. 11, 15, and 16. We use a random spatial distribution of localized states and calculate the corresponding energies with respect to the distribution function  $g_{\epsilon_0}(E)$  using a characteristic energy scale  $\epsilon_0$  which represents the low energy tail of the DOS. The total decay rate of the site  $i$  is given by  $\nu_i = \sum_j \nu_{ij} + \tau_0^{-1}$ , where  $\tau_0$  is the lifetime of an electron-hole pair and  $\nu_{ij}$  the hopping rate from the site  $i$  to the site  $j$ .

Generally, a two-scale model is required to adequately describe the complex Ga(AsBi) system.<sup>11,16–18</sup> These two disorder scales are attributed (i) to spatially extended alloy fluctuations and (ii) to the presence of Bi-clusters.<sup>2,19</sup> After the excitation, the electron-hole pairs perform hopping transitions on the scale of the alloy disorder described by the parameters  $N_1 \alpha_1^2$  and  $\nu_1 \tau_1$ . Here,  $N_1$  is the areal DOS and  $\tau_1$  is the relaxation time to the cluster sites. Their DOS is Gaussian-shaped with a characteristic energy scale of  $\epsilon_1$ , confirmed by absorption measurements.<sup>4</sup> The attempt-to-escape frequency  $\nu_1$  is a measure for the hopping probability and  $\alpha_1$  is the excitonic Bohr radius. Next, the electron-hole pairs relax into the cluster sites, perform hopping transitions between them, and finally recombine with an effective lifetime  $\tau_2$ . This mechanism is described by the second parameter set  $\nu_2 \tau_2$  and  $N_2 \alpha_2^2$  as well as an exponential DOS.  $N_2$ ,

<sup>a)</sup>Electronic mail: sebastian.imhof@physik.tu-chemnitz.de.

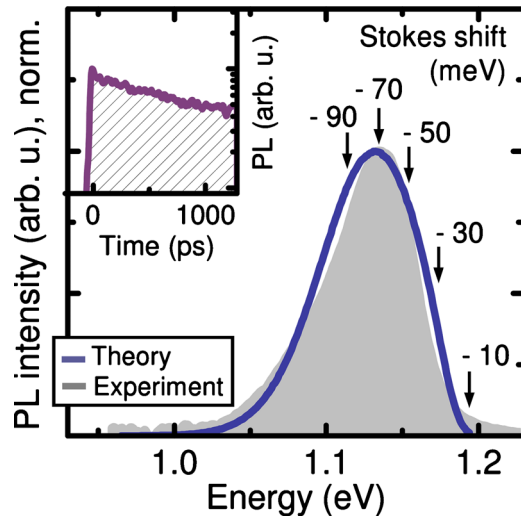


FIG. 1. (Color online) Measured and calculated time-integrated PL spectra of the Ga(AsBi) sample at  $T=10$  K are shown by the gray area and the solid line, respectively. The inset shows the decay of the measured spectrally-integrated PL intensity.

$\nu_2$ , and  $\alpha_2$  are defined analogously to the parameters of the first scale.

An exemplary comparison of the measured and calculated PL spectra for a lattice temperature of 10 K is shown in Fig. 1. Altogether, the temperature dependent PL peak positions and the PL line widths of the Ga(AsBi) sample are correctly reproduced by our model, confirming the two-scale approach.<sup>4</sup>

The corresponding time-resolved data as well as the simulated results are plotted in the left and right hand side of Fig. 2, respectively. The PL intensity is shown in false colors as function of energy (horizontal axis) and time (vertical axis). Again, we obtain an excellent agreement between the simulation and the experiment for all times and energies.

For further analysis of the dynamics the calculated and measured data are integrated across  $\pm 10$  meV for different emission energies and are plotted in Fig. 3. The central spectral positions of the transients are indicated by the arrows in Fig. 1 together with the corresponding Stokes shift, i.e., the difference between the absorption edge and the emission energy  $E_{\text{PL}} - E_{\text{gap}}$ . The data show a short PL lifetime on the high energy side and a long one on the low energy tail typical for disorder-dominated emission decay at low tempera-

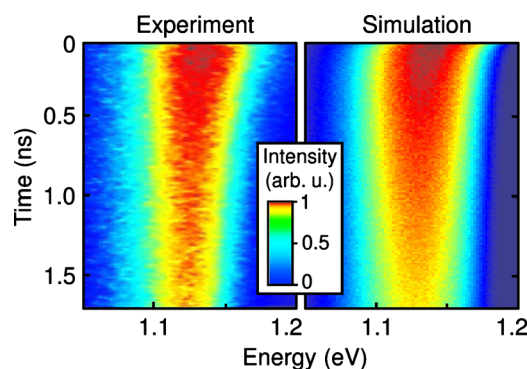


FIG. 2. (Color online) Intensity plots of the measured and simulated PL of the Ga(AsBi) sample at  $T=10$  K are shown on the left- and the right hand side, respectively. The horizontal axis represents the energy scale, the vertical axis the time after the excitation.

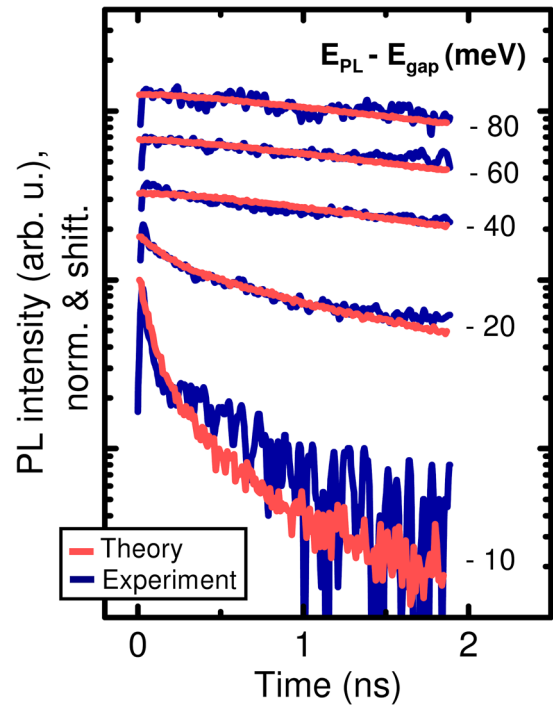


FIG. 3. (Color online) Measured and calculated PL transients at  $T=10$  K for Stoke's shift energies  $E_{\text{PL}} - E_{\text{gap}}$  of  $-10$ ,  $-30$ ,  $-50$ ,  $-70$ , and  $-90$  meV from bottom to top.

tures. The dynamics of carriers at the high energy flank is dominated by hopping to states with lower energy. The electron-hole pairs on the low energy side are trapped in localized states and decay slowly with  $\tau_2$ . Additionally, localized low energy states get filled by carriers from energetically higher sites resulting in a further reduction in the effective decay rate on the low energy tail of the PL.

The comparison of experimental and modeled data now allows for the extraction of the disorder parameters. We find an energy scale for the alloy disorder (Gaussian distribution) of  $\epsilon_1=45$  meV and  $\epsilon_2=11$  meV for the cluster sites (exponentially distributed DOS). The product  $N_2\alpha_2^2$  is correlated with the excitation power in the experiment. It is thus set to 0.15 for an excitation power of 3 mW, corresponding to the photon flux of  $4 \times 10^{12}$   $\text{cm}^{-2} \text{s}^{-1}$ , also consistent with the values used in Ref. 11. The additional information from the PL dynamics allows us to determine the parameters  $\tau_2$  and  $\nu_2$  individually, and not just the product  $\tau_2\nu_2$ . Furthermore, the upper limits for the parameters  $\tau_1$  and  $\nu_1$  are established. We obtain an attempt-to-escape frequency on the alloy disorder scale  $\nu_1=10^{14}$   $\text{s}^{-1}$  and a relaxation time to the cluster scale of  $\tau_1=5 \times 10^{-12}$  s as well as  $\nu_2=2.5 \times 10^{12}$   $\text{s}^{-1}$  and  $\tau_2=4 \times 10^{-9}$  s for the effective lifetime of an electron-hole pair. Thus, the hopping rates are generally faster for the first, alloy-fluctuations-disorder scale than for the transitions between the individual cluster sites. Also, the average capture time  $\tau_1$  of 5 ps to a Bi cluster is significantly smaller than the effective lifetime  $\tau_2$  of an electron-hole pair in the ns range. It should be noted that all time-resolved experimental data are reproduced using the parameters from the time-integrated study in Ref. 11.

Finally, the deduced  $1/e$ -decay times of the measured and calculated PL transients are plotted as function of the emission energy in Fig. 4. Consistently, we obtain decay-times at higher energies which are much shorter than the

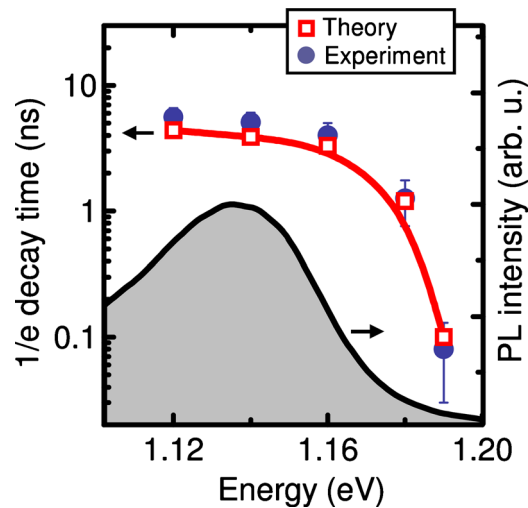


FIG. 4. (Color online) Measured and calculated  $1/e$ -decay times for a lattice temperature of  $T=10$  K. The time-integrated measured PL spectrum is given by the gray-shaded area as a reference.

lifetime  $\tau_2$  while the values on the low energy side are slightly above  $\tau_2$ , indicating additional filling effects.

In summary, the spectral and temporal dependencies of the PL decay of the Ga(AsBi) sample are investigated by time-resolved PL and analyzed using kinetic Monte Carlo simulations. This simulation technique gives access to the absolute energy scale on the low energy tail of the DOS. In addition the few disorder parameters have physical interpretations, e.g.,  $\tau_2$  represents the excitonic lifetime of the cluster states. The experimental data show typical disorder-induced effects, namely a fast decay on the high energy side of the PL spectrum and much longer decay at lower energies, attributed to the relaxation, and recombination-dominated dynamics, respectively. The simulations correctly reproduce the experimental findings using a two-scale hopping model consistent with the previous studies. The experiment-theory comparison of the time-dependent data yields a complete set of the individual disorder parameters of the cluster sites. Further, an upper boundary is established for the average capture time into the Bi cluster sites. Both findings cannot be

achieved by the analysis of time-integrated data only.

We gratefully acknowledge financial support through the Materials World Network: III–V Bismide Materials for IR and Mid IR Semiconductors.

- <sup>1</sup>S. Tixier, M. Adamczyk, T. Tiedje, S. Francoeur, A. Mascarenhas, P. Wei, and F. Schiettekatte, *Appl. Phys. Lett.* **82**, 2245 (2003).
- <sup>2</sup>S. Francoeur, M.-J. Seong, A. Mascarenhas, S. Tixier, M. Adamczyk, and T. Tiedje, *Appl. Phys. Lett.* **82**, 3874 (2003).
- <sup>3</sup>W. Huang, K. Oe, G. Feng, and M. Yoshimoto, *J. Appl. Phys.* **98**, 053505 (2005).
- <sup>4</sup>S. Imhof, C. Bückers, A. Thränhardt, J. Hader, J. V. Moloney, and S. W. Koch, *Semicond. Sci. Technol.* **23**, 125009 (2008).
- <sup>5</sup>K. Alberi, J. Wu, W. Walukiewicz, K. M. Yu, O. D. Dubon, S. P. Watkins, C. X. Wang, X. Liu, Y.-J. Cho, and J. Furdyna, *Phys. Rev. B* **75**, 045203 (2007).
- <sup>6</sup>B. Fluegel, S. Francoeur, A. Mascarenhas, S. Tixier, E. C. Young, and T. Tiedje, *Phys. Rev. Lett.* **97**, 067205 (2006).
- <sup>7</sup>A. Janotti, S.-H. Wei, and S. B. Zhang, *Phys. Rev. B* **65**, 115203 (2002).
- <sup>8</sup>X. Lu, D. A. Beaton, R. B. Lewis, T. Tiedje, and Y. Zhang, *Appl. Phys. Lett.* **95**, 041903 (2009).
- <sup>9</sup>G. B. Stringfellow, *Organometallic Vapor-Phase Epitaxy*, Theory and Practice, 2nd ed. (Academic, New York, 1989).
- <sup>10</sup>S. D. Baranovskii, R. Eichmann, and P. Thomas, *Phys. Rev. B* **58**, 13081 (1998).
- <sup>11</sup>S. Imhof, A. Thränhardt, A. Chernikov, M. Koch, N. S. Köster, K. Kolata, S. Chatterjee, S. W. Koch, X. Lu, S. R. Johnson, D. A. Beaton, T. Tiedje, and O. Rubel, *Appl. Phys. Lett.* **96**, 131115 (2010).
- <sup>12</sup>O. Rubel, W. Stolz, and S. D. Baranovskii, *Appl. Phys. Lett.* **91**, 021903 (2007).
- <sup>13</sup>O. Rubel, M. Galluppi, S. D. Baranovskii, K. Volz, L. Geelhaar, H. Riechert, P. Thomas, and W. Stolz, *J. Appl. Phys.* **98**, 063518 (2005).
- <sup>14</sup>O. Rubel, S. D. Baranovskii, K. Hantke, B. Kunert, W. W. Rühle, P. Thomas, K. Volz, and W. Stolz, *J. Lumin.* **127**, 285 (2007).
- <sup>15</sup>A. Miller and E. Abrahams, *Phys. Rev.* **120**, 745 (1960).
- <sup>16</sup>S. Imhof, A. Chernikov, M. Koch, K. Kolata, N. S. Köster, S. Chatterjee, S. W. Koch, X. Lu, S. R. Johnson, D. A. Beaton, T. Tiedje, O. Rubel, and A. Thränhardt, *Phys. Status Solidi B* **248**, 851 (2010).
- <sup>17</sup>K. Kazlauskas, G. Tamulaitis, Z. Zukauskas, M. A. Khan, J. W. Yang, J. Zhang, G. Simin, M. S. Shur, and R. Gaska, *Appl. Phys. Lett.* **83**, 3722 (2003).
- <sup>18</sup>C. Karcher, K. Jandieri, B. Kunert, R. Fritz, M. Zimprich, K. Volz, W. Stolz, F. Gebhardt, S. D. Baranovskii, and W. Heimbrodt, *Phys. Rev. B* **82**, 245309 (2010).
- <sup>19</sup>G. Ciatto, E. C. Young, F. Glas, J. Chen, R. A. Mori, and T. Tiedje, *Phys. Rev. B* **78**, 035325 (2008).